

# High-Frequency Bistatic Scattering by Depolarizing, Nearly Omnidirectional Reflectors: Higher Order Polyhedral Reflectors

Gildas Kubické, *Student Member, IEEE*, Christophe Bourlier, *Member, IEEE*, and Joseph Saillard

**Abstract**—The bistatic scattering by perfectly conducting higher order polyhedral reflectors of large dimensions with respect to the wavelength, is studied. These particular faceted polyhedra, composed of several identical trihedral corner reflectors (TCR), are expected to exhibit a large RCS over a wide angular range with specific properties in terms of directivity and depolarization. Since numerical methods can not be applied to these complex structures (owing to the number of unknowns involved), an asymptotic method based on the physical optics combined with the geometrical optics approximations and the method of equivalent currents, recently developed for a single TCR, is used. The validity of the extended method is discussed and results for higher order (first-, second- and fourth-order) octahedral reflectors and icosahedral reflectors are also studied, in particular in terms of depolarization.

**Index Terms**—Corner reflectors, diffraction, electromagnetic scattering, geometrical optics (GOs), physical optics (POs), radar cross section (RCS).

## I. INTRODUCTION

THIS PAPER IS devoted to the study of a group of radar reflectors: the polyhedral corner reflectors. For clarification, let us introduce the following acronyms:

- Double reflection (DR).
- Geometrical optics (GO).
- Icosahedral reflector (IR).
- Method of equivalent currents (MEC).
- Multilevel fast multipole method (MLFMM).
- Octahedral reflector (OR).
- Physical optics (PO).
- Radar cross section (RCS).
- Single diffraction (SD).
- Single reflection (SR).
- Trihedral corner reflector (TCR).
- Triple reflection (TR).

Reflectors, which present a nearly omnidirectional RCS and a specific depolarization, are needed for many applications concerning radar systems. As a consequence, an ideal omnidirectional radar reflector reflects incident waves uniformly in all directions and takes the form of a sphere. Unfortunately, the

Manuscript received September 14, 2007; revised May 13, 2008. Published September 4, 2008 (projected).

The authors are with the Institut de Recherche en Electrotechnique et Electronique de Nantes Atlantique (IREENA) Laboratory, Ecole polytechnique de l'université de Nantes, 44306 Nantes, cedex 3 France (e-mail: gildas.kubicke@univ-nantes.fr).

Color versions of one or more of the figures in this paper are available online at <http://ieeexplore.ieee.org>.

Digital Object Identifier 10.1109/TAP.2008.928779

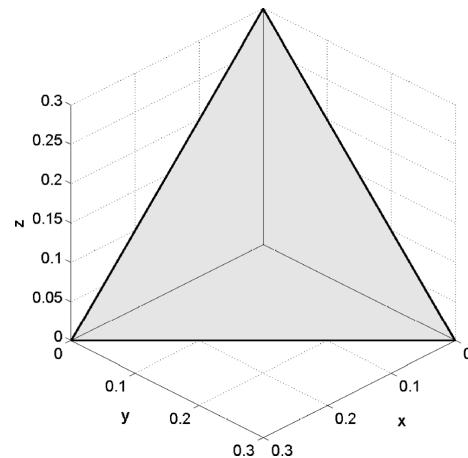


Fig. 1. The trihedral corner reflector.

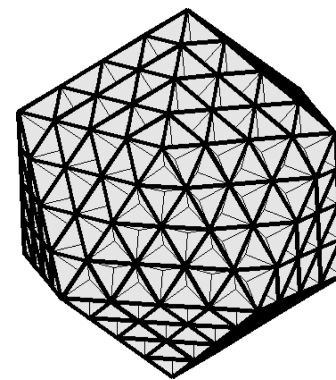


Fig. 2. A polyhedral reflector conforming to a quasi-spherical shape.

convex reflective surface of a spherical reflector does not provide a high RCS.

Contrary to the sphere, it is well known that the TCR, as depicted in Fig. 1, exhibits a large RCS over a wide angular range. Indeed, this is due to DR and TR contributions which provide a return of the incident wave in several directions. Therefore, this reflector is employed as a radar enhancement device and as a practical benchmark target for RCS measurements. It has also been employed as a ground marker target for the calibration of synthetic aperture radar (SAR) images [1], [2]. In spite of the fact that the TCR provides a high and relatively flat backscattering co-polarization response, as a function of incidence angle, the cross-polarization one is lower. Moreover, a high RCS dynamics is obtained. Finally, this reflector can be used in a restricted angular domain, i.e., in the interior region which delimits a solid

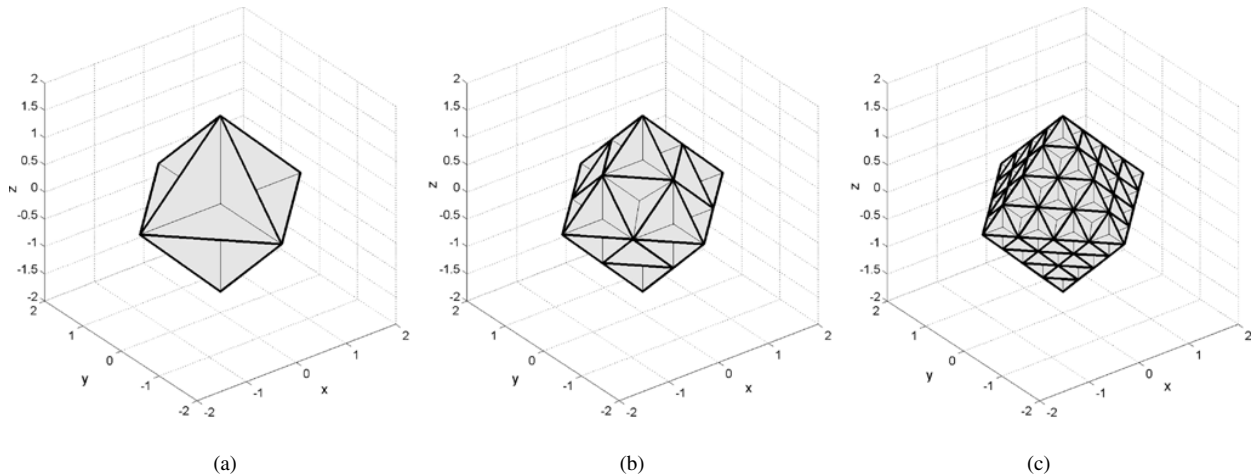


Fig. 3. Higher order octahedral reflectors. (a) First order. (b) Second order. (c) Fourth order.

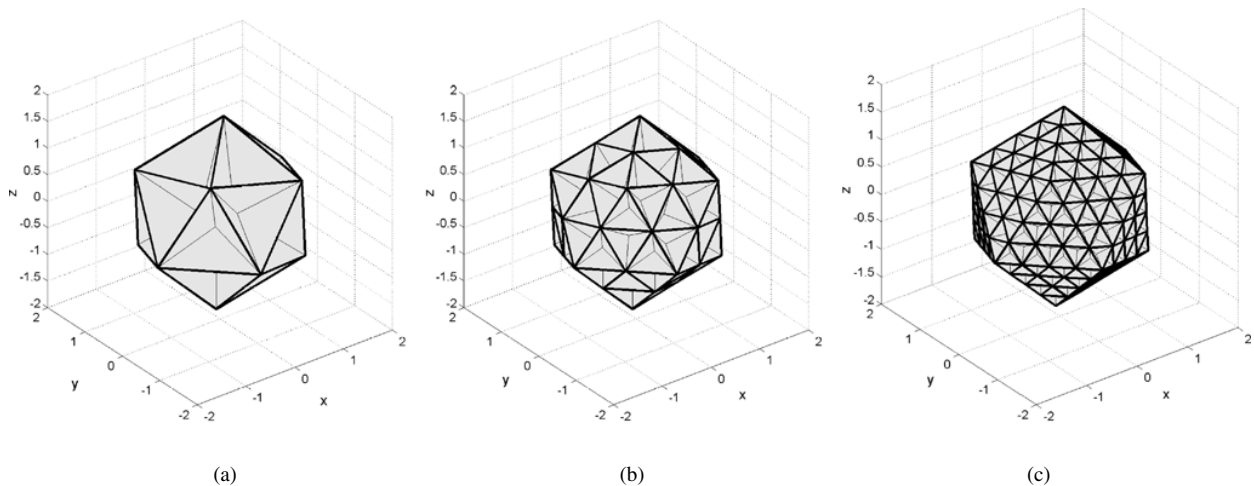


Fig. 4. Higher order icosahedral reflectors. (a) First order. (b) Second order. (c) Fourth order.

angle of  $\pi/2$  steradians. Intuitively, it seems to be interesting to put together many TCRs in order to obtain a  $4\pi$ -steradian response with a high RCS. This kind of reflector should be more appropriate than the TCR for many applications as a radar target for meteorological balloons tracking [3], [4], identifying the position of a person which is in distress [5], mounted on buoys or on a high tower to mark shoals and warn airplanes respectively [6], as a reference target for bistatic polarimetric measurements. The basic idea of this paper is to study a target composed of elementary TCRs located in such manner to tend to a quasi-spherical shape. In the electromagnetic point of view, such a target is expected to present the isotropic sphere property and a local high RCS for each TCR, which leads to a high RCS in  $4\pi$  steradians for this kind of target. An example of such a reflector is presented in Fig. 2. Some U.S. patents describe the usefulness of these reflectors without demonstration [7]–[9].

Indeed, by using high-frequency methods, the bistatic scattering by higher order polyhedral reflectors has not been evaluated yet.

Let us introduce the geometry of these structures. A polyhedral reflector is a polyhedron for which each face is replaced by a TCR. This corresponds to a first-order polyhedral reflector.

A polyhedral reflector of order  $N$  is a polyhedral reflector in which each elementary TCR of internal length  $L$  is replaced by a TCR array, for which each TCR has an internal length equal to  $L/N$ . For instance, see Figs. 3(a) and 4(a) for the first-order OR (initially this polyhedron has eight faces) and IR (initially this polyhedron has 20 faces) respectively. If  $N = 2$ , the number of TCRs equals 32 and 80 for the second-order OR and IR, respectively. In Fig. 3(b) and (c) the second-order and fourth-order ORs are depicted, and in Fig. 4(b) and (c) the second-order and fourth-order IRs are depicted. From the geometry of the polyhedral reflector [10], the local basis  $(\hat{u}_{x_i}, \hat{u}_{y_i}, \hat{u}_{z_i})$  related to the elementary TCR which is numbered  $i = 1 \dots n$  ( $n = 8 \times N^2$  for OR and  $n = 20 \times N^2$  for IR), is expressed in the global coordinate system.

Then, the bistatic scattering by the polyhedral reflector is computed by using an analytical asymptotic method, presented in details in [11], [12]. This method evaluates (by using PO, GO, and MEC) the bistatic scattering by TCR and for any excitation and observation angles. It is a generalization to the bistatic full-polarimetric case of the calculus of Corona *et al.* [13] and Polycarpou *et al.* [14], which studied the monostatic scattering of a TCR when it is excited and observed in the interior re-

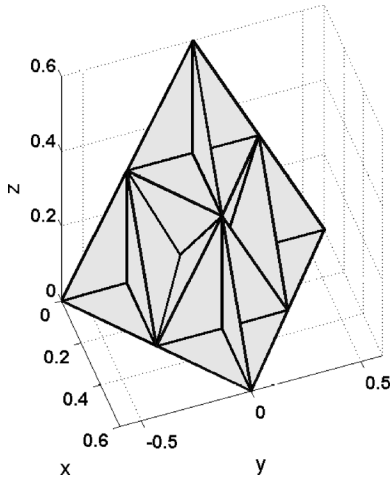


Fig. 5. A part of the second-order octahedral reflector (only two faces replaced by second-order TCR arrays).

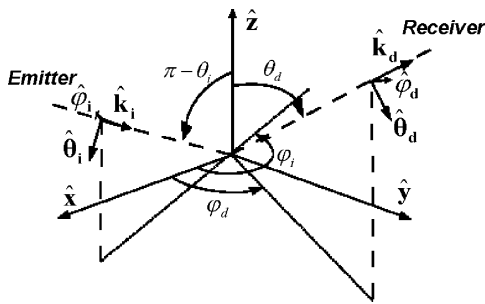


Fig. 6. Angles in FSA convention.

gion. To be consistent with the PO, coupling effects between the TCRs of the polyhedral reflector are not taken into account, and the method described in [12] is applied for each TCR. Then, all bistatic scattering matrices are transposed in the global coordinate system by using the spherical and Euler rotation matrices (and a phase translation if necessary). Finally, a coherent summation is realized.

This method was applied for a first-order octahedral reflector in [12] and comparisons with a numerical method (MLFMM) showed very good results. In [15], the method was applied for a first-order icosahedral reflector and comparisons with the first-order OR showed that the OR is more directive than the IR.

In this paper, the method proposed in [12], is extended for more complex structure: the higher order polyhedral reflector in order to reveal some important radar scattering properties.

First, comparisons are made between the asymptotic method and the MLFMM, obtained from FEKO software [16], [17]. Indeed, even if the proposed method provided good results with the benchmark method in [11], [12], [15], the method have never been tested for more complex structure in which the TCRs are not located as in the first-order OR, and can present effects which are not taken into account (as coupling effect between TCRs, double diffraction or diffraction reflection for example). The validity of the approach is discussed in monostatic and bistatic cases, and the method is tested with a small reflector (comparately with the wavelength) in order to test the limit of

validity of the method. Finally, results in terms of depolarization behaviour are discussed in order to reveal property of the higher order polyhedral reflectors.

## II. COMPARISON WITH THE MLFMM

First, the monostatic RCS of a single TCR was compared with the results of [13], [14] (no simulation was presented for cross-polarizations) for co-polarizations. A perfect agreement is observed, which permits to validate the contribution computations obtained from the GO, PO and MEC approximations for a single TCR. In addition, in [12], for the case of the first-order OR and for monostatic and bistatic configurations, the proposed method was compared with the benchmark MLFMM obtained from FEKO software [17]. A good agreement is observed for co-polarizations, which shows that the blockage effects (shadowing effect in excitation and observation) must be taken into account. On the other hand, some differences were observed for cross-polarizations.

In this paper, owing to the number of unknowns involved for the MLFMM, the validity of the method is tested for a quarter second-order OR (see Fig. 5). For the MLFMM, the sampling step is taken as  $\lambda/5$  (personal computer: CPU Intel Pentium 4 at 2.4 GHz and 2Go of RAM) owing to computer memory restrictions (80 504 unknowns).

### A. Monostatic Configuration

One of the advantages of the proposed method is that each component contributing to the total signature can be evaluated separately. In Fig. 7, the RCSs  $\sigma_{\theta\theta}$  and  $\sigma_{\phi\theta}$  are plotted versus the observation angle  $\theta_d$  for  $\phi_d = \pi/6$  in the monostatic configuration ( $\theta_i = \pi - \theta_d$ ,  $\phi_i = \pi + \phi_d = 7\pi/6$ ) for different contributions. The inner edge length  $L$  of each TCR of the structure, is equal to  $10\lambda$  with a frequency of 10 GHz. Angles  $\theta_i$ ,  $\phi_i$ ,  $\theta_d$  and  $\phi_d$  are defined in FSA convention as depicted in Fig. 6.

As one can see, there is an excellent agreement between the benchmark method and the “full” proposed method (SR+DR+TR+MEC) in co-polarization. In cross-polarization, a good agreement is observed around the maximum value, and as the observation angle deviates from the direction of maximum value, the difference increases. Other simulations with different values of the azimuth incidence angle ( $\phi_i = \{\pi, 3\pi/2\}$ ) and not presented in this paper, lead to the same conclusion.

The differences can be attributed to the diffraction/reflection contributions which are not taken into account in the proposed method. A solution could be the iteration of the MEC and the PO, but the computation time would increase if the interaction is computed in near field, because the triple integrals could not be solved analytically. Another approach, like the geometrical theory of diffraction (GTD) [18], [19], could be applied instead of the GO for the first reflections during the DR and TR. This would take into account the interaction between faces as the GO does, but also the interactions between edges and faces with a “reasonable increase of the computer time” as said by Corona *et al.* [20]. It is important to note that under the GO approximation, the scattered wave is assumed to be a plane wave between two successive reflections. This assumption avoids quadruple integrals for DR, and sextuple integrals for TR. But this can alter the results, notably for cross-polarizations. This assumption is

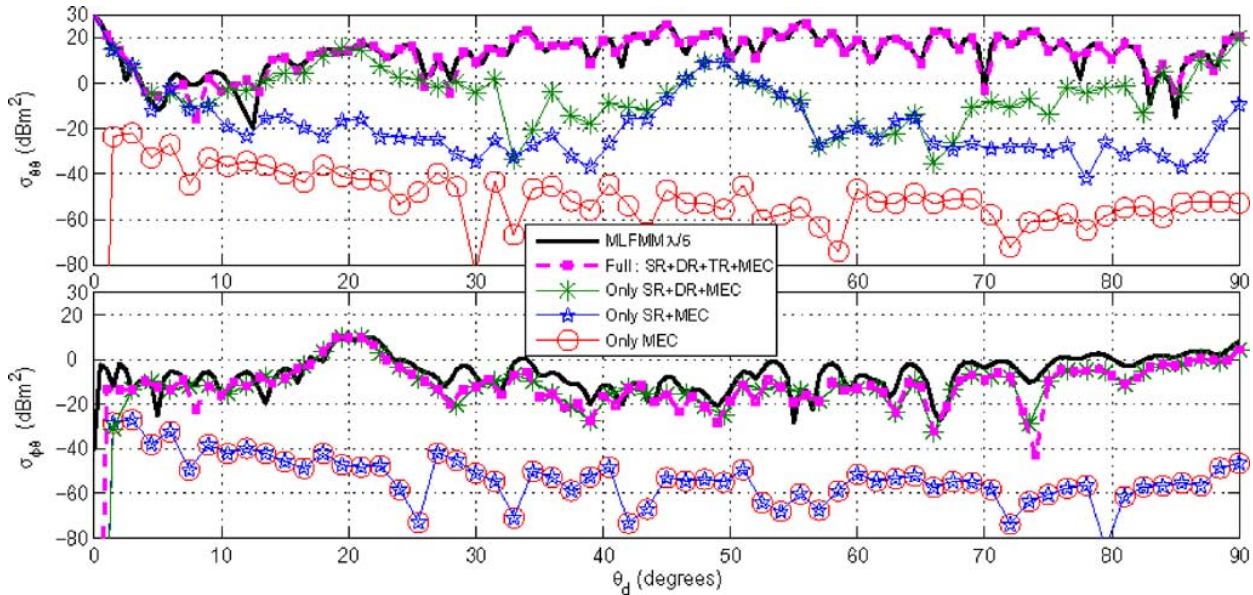


Fig. 7. Co- (top) and cross- (bottom) polarizations: monostatic RCSs of the quarter second-order OR versus  $\theta_d$  ( $\phi_d = \pi/6$ ,  $L = 10\lambda$ ,  $f = 10$  GHz).

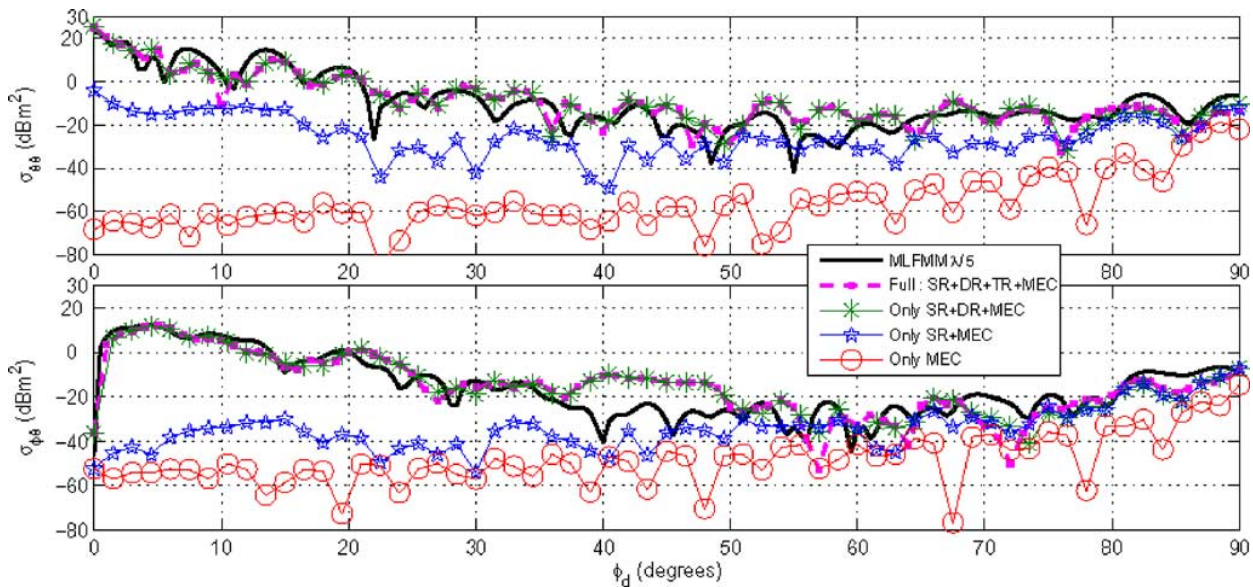


Fig. 8. Co- (top) and cross- (bottom) polarizations: bistatic RCSs of the quarter second-order OR versus  $\phi_d$  (with  $L = 10\lambda$ ,  $f = 10$  GHz,  $\theta_i = 2\pi/3$ ,  $\theta_d = \pi/3$  and  $\phi_i = \pi$ ).

discussed in details by Griesser *et al.* [21] for a dihedral corner reflector.

In Fig. 7, one can observe that the MEC provides low values in comparison with the other contributions. Indeed, in cross-polarizations, the DR provides high values (SR+DR+MEC compared to SR+MEC), whereas the TR is negligible (SR+DR+TR+MEC compared to SR+DR+MEC). However, the TR contribution must be included in co-polarizations. In fact, the MEC is generally necessary for the co- and cross-polarizations if the other contributions provide values of the same order of magnitude.

### B. Bistatic Configuration

In Fig. 8, the RCSs  $\sigma_{\theta\theta}$  and  $\sigma_{\phi\theta}$  are plotted versus the observation angle  $\phi_d$  for a bistatic configuration ( $\theta_i = 2\pi/3$ ,

$\theta_d = \pi/3$  and  $\phi_i = \pi$ ) for different contributions. The target and the frequency are the same as the ones used for the monostatic configuration (Section II-A).

As one can see, there is a good agreement between the benchmark method and the “full” proposed method (SR+DR+TR+MEC) in co- and cross- polarizations. Nevertheless, around  $\phi_d = 45^\circ$  in cross-polarization, the differences increase. Indeed, it can be shown that this overestimation is related to the overprediction of the double reflection contribution occurring in the two returned TCRs. In conclusion, the slight differences can be attributed to the reasons already mentioned for the monostatic configuration (Section II-A). But it is important to notice that, obviously, for bistatic calculations there are additional blockage effects due to the

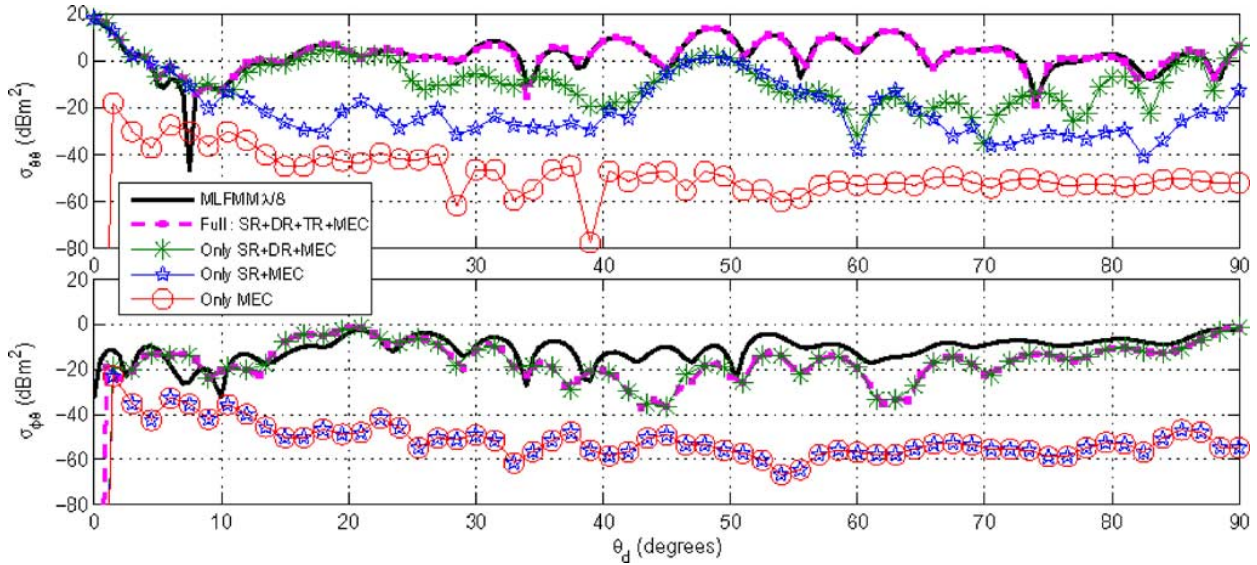


Fig. 9. Co- (top) and cross- (bottom) polarizations: monostatic RCSs of the quarter second-order OR versus  $\theta_d$  ( $\phi_d = \pi/6$ ,  $L = 5\lambda$ ,  $f = 10$  GHz).

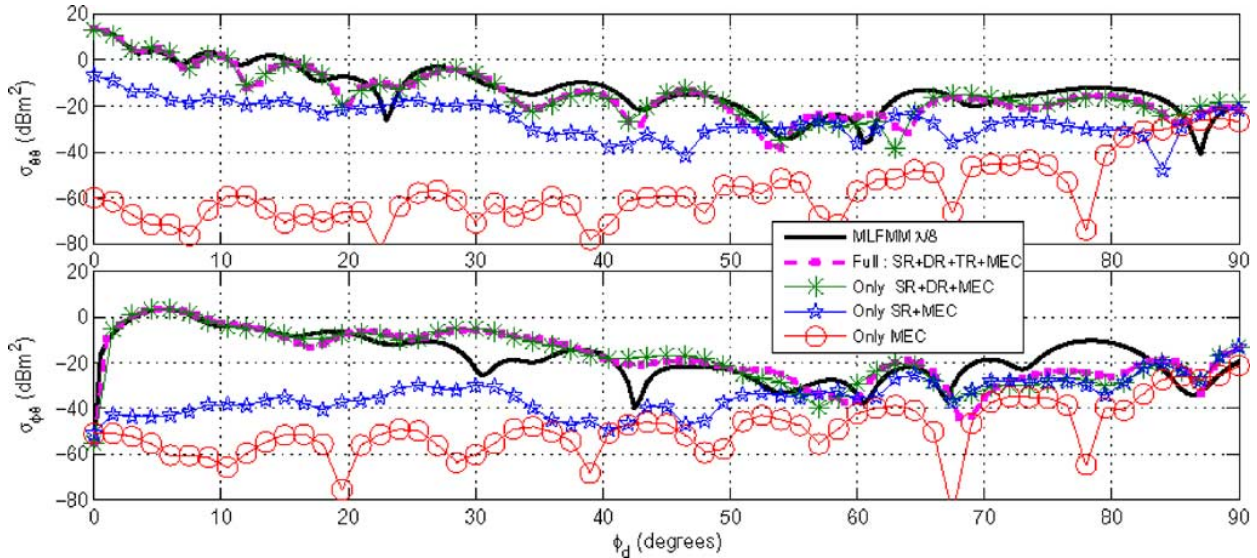


Fig. 10. Co- (top) and cross- (bottom) polarizations: bistatic RCSs of the quarter second-order OR versus  $\phi_d$  (with  $L = 5\lambda$ ,  $f = 10$  GHz,  $\theta_i = 2\pi/3$ ,  $\theta_d = \pi/3$  and  $\phi_i = \pi$ ).

separation of source and observation. Consequently, the GO limits can be more revealed.

### C. Monostatic Case With a Small Reflector

In Fig. 9, the RCSs  $\sigma_{\theta\theta}$  and  $\sigma_{\phi\theta}$  are plotted versus the observation angle  $\theta_d$  with the same parameters as in Section II-A, but with an internal edge length  $L$  equal to  $5\lambda$ . This means that the reflector may not be in the high frequency domain, in order to test the accuracy of our asymptotic approach according to electrical size. The sampling step for the MLFMM is taken as  $\lambda/8$  since the reflector is smaller than the one studied in Section II-A.

These results can be compared with the ones in Fig. 7, where  $L$  is equal to  $10\lambda$ . As one can see, there is a very good agreement in co-polarization, whereas discrepancies appear in cross-polarization. These differences are bigger than the ones obtained in

Section II-A. In conclusion, even though PO and GO approximations may be inappropriate for this configuration, results for the co-polarization case are quite accurate but less accurate for the cross-polarization case.

### D. Bistatic Case With a Small Reflector

In Fig. 10, the RCSs  $\sigma_{\theta\theta}$  and  $\sigma_{\phi\theta}$  are plotted versus the observation angle  $\phi_d$  with the same parameters as in Section II-B but with an internal edge length  $L$  equal to  $5\lambda$ .

These results can be compared with the ones in Fig. 8, where  $L$  is equal to  $10\lambda$ . As one can see, there is a quite good agreement in co-polarization. In cross-polarization, our model gives good results near the backscattering angle ( $\phi_d = 0^\circ$ ). The discrepancies in cross-polarization are bigger than those obtained in Section II-B.

TABLE I  
COMPUTATION TIME REQUIRED, BY THE PROPOSED METHOD AND THE MLFMM, TO OBTAIN THE FOUR COMPONENTS OF THE SCATTERING MATRIX

	Our method	MLFMM
Fig. 7	4.8 seconds	53 hours 10 minutes
Fig. 8	3 seconds	33 minutes
Fig. 9	3.6 seconds	10 hours 58 minutes
Fig. 10	2.4 seconds	24 minutes

Thus, one can say that the internal edge length  $L$  of the reflectors must be at least equal to  $10\lambda$  in order to obtain good results both in co- and cross-polarizations.

One of the advantages of the proposed method is the computation time. In Table I the computation time, required to obtain the four components of the scattering matrix, for the MLFMM and our method, is given for each configuration studied before (Sections II-A–II-D). In conclusion, the proposed method is very interesting for real-time applications.

### III. PROPERTIES OF THE HIGHER-ORDER POLYHEDRAL REFLECTORS

A comparison was made between the first-order OR and the first-order IR in [15]. For the OR, the response of each TCR (eight) that composes the OR slightly interferes with the neighbour TCRs. Indeed, the solid angle of each TCR ( $\pi/2$  steradians) does not overlap with the solid angle of other TCRs. Thus, high RCS values are obtained for each TCR near the specular directions (TR, DR and SR specular directions). Finally, it was demonstrated that the class of the polyhedral reflector modifies the directivity since it was shown that the OR is more directive than the IR. Let us now focus on the effects of the reflector order.

In order to compare the first-, second-, and fourth-order ORs and IRs, the objects are chosen with the same global dimensions [Figs. 3(a)–4(c)]. For all these reflectors, the circumscribed sphere has a radius of 1.614 m. For example, the inner edge length of a TCR of the fourth-order IR equals 0.3 m, which equals  $10\lambda$  for  $f = 10$  GHz. Thus, each TCR is in the high-frequency domain.

Let us introduce the cumulative function computed as follows: the number of values ranging between two given RCS values (histogram) is calculated. For a given threshold ranging from  $\min(\text{RCS})$  to  $\max(\text{RCS})$ , the cumulative function is obtained by integrating the histogram between  $\min(\text{RCS})$  and the threshold. In addition, the cumulative function is normalized, such that its final value [which occurs at  $\max(\text{RCS})$ ] equals one. In fact, for any value  $\sigma$ , the cumulative function value corresponds to the fraction of the data that is strictly smaller than  $\sigma$ .

Figs. 11 and 12 compare the ratio  $\sigma_{\theta\theta}/\sigma_{\phi\theta}$  (in decibel scale) in terms of cumulative function by considering the first-, second-, and fourth-order ORs (Fig. 11) and IRs (Fig. 12). As the order increases, the curves are shifted toward the left, which means that  $\sigma_{\theta\theta}(\text{dBm}^2) - \sigma_{\phi\theta}(\text{dBm}^2)$  decreases. This implies that the fourth-order polyhedral reflector is more depolarizing than the first- and second-order polyhedral reflectors, since the difference between the cross- and co-polarization values decreases when the order increases. For example, for the fourth-order IR in Fig. 12, 50% of the values are smaller than 10 dB, which means that the co-polarization values are at most 10 dB higher than the cross-polarization values for 50%

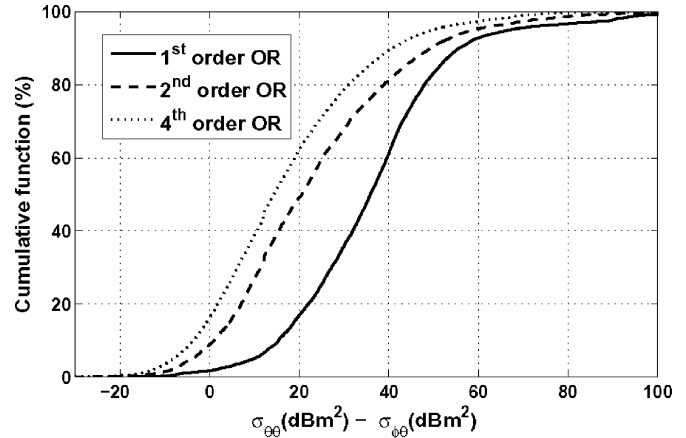


Fig. 11. Cumulative function of  $\sigma_{\theta\theta}(\text{dBm}^2) - \sigma_{\phi\theta}(\text{dBm}^2)$  for higher order ORs.

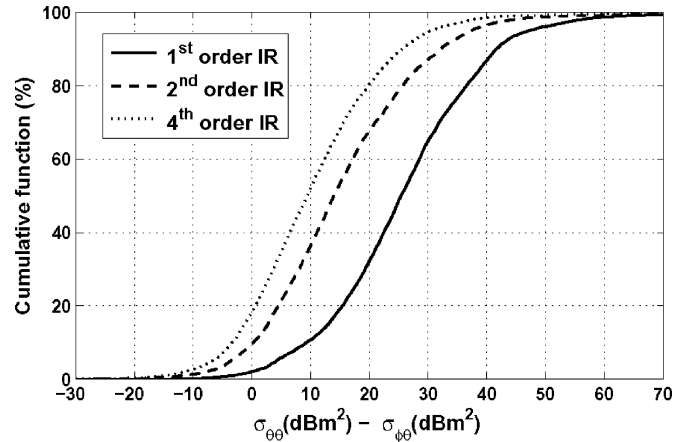


Fig. 12. Cumulative function of  $\sigma_{\theta\theta}(\text{dBm}^2) - \sigma_{\phi\theta}(\text{dBm}^2)$  for higher order IRs.

of monostatic configurations. In conclusion, the depolarization effect is improved when the order of the polyhedral reflector increases.

### IV. CONCLUSION

In this paper, a fast asymptotic method (based on PO, GO and MEC) is applied for higher order polyhedral reflectors in order to study their radar scattering properties. First, comparisons with a benchmark method are made to study the validity of the method when it is applied on these particular complex structures. This leads to excellent agreement for co-polarization, whereas for the cross-polarization, differences are observed and discussed. Indeed, some improvements can be added by computing other components, like the diffraction/reflection contributions and the coupling effect between faces during DR and TR in near-field zone. The proposed method permits to compute the full bistatic RCS of a very complex scene composed of several large polyhedral reflectors in a very short computation time, which is very interesting for real-time systems.

It was demonstrated in a recent communication [15] that when the class (number of elementary TCRs of the first order) of the polyhedral reflector increases, the reflector better approximates the sphere shape. Thus, a nearly omnidirectional

reflector can be obtained by increasing the class, and the high RCS values of TCRs are kept. In this paper, the study leads to a new conclusion: when the order increases, the depolarization increases, which provides another depolarizing effect that the one described in [22]–[24].

#### ACKNOWLEDGMENT

The authors would like to thank Dr. P. Pouliguen (Délégation Générale pour l'Armement, CELAR, Bruz, France) for his judicious advice.

#### REFERENCES

- [1] J. van Zyl, "Calibration of polarimetric radar images using only image parameters and trihedral corner reflector responses," *IEEE Trans. Geosci. Remote Sensing*, vol. 28, pp. 337–48, May 1990.
- [2] C. Bradley, P. Collins, J. Fortuny-Guasch, M. Hastriter, G. Nesti, A. J. Terzuoli, Jr, and K. Wilson, "An investigation of bistatic calibration objects," *IEEE Trans. Geosci. Remote Sensing*, vol. 43, pp. 2177–84, Oct. 2005.
- [3] P. Eccles, "The orientation and construction of high efficiency passive radar targets," *Proc. IEEE*, vol. 53, pp. 1115–1117, Aug. 1965.
- [4] J. Laby and J. Sparrow, "Wind studies using level balloons," *J. Appl. Meteorol.*, vol. 4, pp. 585–589, Oct. 1965.
- [5] G. E. Gentry and J. H. Bain, Jr., "Inflatable Radar Reflector," U.S. Patent 4673934, Jun. 16, 1987.
- [6] E. K. P. Graham, "Reflector for Radar Purposes," U.S. Patent 2763000, Sep. 11, 1956.
- [7] L. van Buskirk, "Radar Significant Target," U.S. Patent 4096479, Jun. 20, 1978.
- [8] R. Berg, "Omni-Directional Radar and Electro-Optical Multiple Corner Retro Reflector," U.S. Patent 4551726, Nov. 5, 1985.
- [9] F. Canning, "Arrangement of Corner Reflectors for a Nearly Omnidirectional Return," U.S. Patent 6742903 B2, Jun. 1, 2004.
- [10] P. Cromwell, *Polyhedra*. Cambridge, U.K.: Cambridge Univ. Press, 1999.
- [11] G. Kubické, C. Bourlier, and J. Saillard, "A physical optics solution for bistatic RCS of triangularly shaped trihedral corners for any incidence and observation angles," in *Proc. EUCAP Conf.*, Nice, France, Nov. 6–10, 2006, pp. 1–6, ref. 347601.
- [12] G. Kubické, C. Bourlier, and J. Saillard, "Polarimetric bistatic signature of a faceted octahedron in high-frequency domain," *Progr. Electromagn. Res.*, vol. 71, pp. 173–209, 2007.
- [13] P. Corona, G. Ferrara, C. Gennarelli, and G. Riccio, "A physical optics solution for the backscattering by triangularly shaped trihedral corners," *Annales des Telecommun.*, vol. 50, no. 5–6, pp. 557–62, May 1995.
- [14] A. Polycarpou, C. Balanis, and C. Birtcher, "Radar cross section of trihedral corner reflectors using PO and MEC," *Annales des Telecommun.*, vol. 50, no. 5–6, pp. 510–16, May 1995.
- [15] G. Kubické, C. Bourlier, and J. Saillard, "Comparison of bistatic signatures of octahedral and icosahedral reflectors in the high-frequency domain," in *Proc. 4th European Radar Conf. EuMA*, Munich, Germany, Oct. 10–12, 2007, pp. 425–428.
- [16] J. van Tonder and U. Jakobus, "Fast multipole solution of metallic and dielectric scattering problems in FEKO," in *Proc. Int. Conf. on Wireless Communications and Applied Computational Electromagnetics IEEE/ACES*, 2005, pp. 511–14.
- [17] FEKO – EM Software and Systems Technopark-Stellenbosch, South Africa [Online]. Available: [www.feko.info](http://www.feko.info)
- [18] J. Keller, "Geometrical theory of diffraction," *J. Opt. Soc. Amer.*, vol. 52, pp. 116–130, 1962.
- [19] R. Kouyoumjian and P. Pathak, "A uniform geometrical theory of diffraction for an edge in a perfectly conducting surface," *Proc. IEEE*, vol. 62, no. 11, pp. 1448–1461, Nov. 1974.
- [20] P. Corona, G. Ferrara, F. D'Agostino, C. Gennarelli, and G. Riccio, "An improved physical optics model for the evaluation of the field backscattered by triangular trihedral corner reflectors," in *Proc. 8th Mediterranean Electrotechnical Conf. on Industrial Applications in Power Systems, Computer Science and Telecommunications (MELECON 96)*, May 1996, vol. 1, pp. 534–537.

- [21] T. Griesser and A. Balanis, "Backscatter analysis of dihedral corner reflectors using physical optics and the physical theory of diffraction," *IEEE Trans. Antennas Propag.*, vol. AP-35, pp. 1137–1147, Oct. 1987.
- [22] D. Michelson and E. Jull, "Depolarizing trihedral corner reflectors for radar navigation and remote sensing," *IEEE Trans. Antennas Propag.*, vol. AP-43, pp. 513–518, May 1995.
- [23] P. Corona, F. D'Agostino, G. Ferrara, C. Gennarelli, and G. Riccio, "Physical optics analysis of the field backscattered by a depolarising trihedral corner reflector," *Inst. Elect. Eng.*, vol. 145, no. 3, pp. 213–218, Jun. 1998.
- [24] H. Hänninen, M. Pitkonen, and K. Nikoskinen, "Method of moments analysis of the backscattering properties of a corrugated trihedral corner reflector," *IEEE Trans. Antennas Propag.*, vol. 54, pp. 1167–1173, Apr. 2006.



**Gildas Kubické** (S'05) was born in Longjumeau, France, on September 28, 1982. He received the Engineering degree and the M.S. degree in electronics and electrical engineering both from the Ecole polytechnique de l'université de Nantes (EpuN), Nantes, France, in 2005, where he is currently working toward the Ph.D. degree.

During his M.S. studies he investigated inverse problems for radar imagery. He is currently a member of the Radar Team in the Institut de Recherche en Electrotechnique et Electronique de

Nantes Atlantique (IREENA) Laboratory, Ecole polytechnique de l'université de Nantes, Nantes, France, where he is working on scattering by an object located above a rough surface, specifically in the high-frequency domain.



**Christophe Bourlier** (M'99) was born in La Flèche, France, on July 6, 1971. He received the M.S. degree in electronics from the University of Rennes, Rennes, France, in 1995 and the Ph.D. degree from the Ecole polytechnique de l'université de Nantes, Nantes France, in 1999

While at the University of Rennes, he was with the Laboratory of Radiocommunication where he worked on antennas coupling in the VHF-HF band. Now, he is with Radar Team in the Institut de Recherche en Electrotechnique et Electronique de

Nantes Atlantique (IREENA) Laboratory, Ecole polytechnique de l'université de Nantes, Nantes France. He works as an Assistant Researcher at the National Center for Scientific Research on electromagnetic wave scattering from rough surfaces and objects for remote sensing applications. He is the author of more than 80 journal articles and conference papers.



**Joseph Saillard** was born in Rennes, France, in 1949. He received the Ph.D. degree and the "Docteur d'Etat" in Physics from the University of Rennes, Rennes, France, in 1978 and 1984, respectively.

From 1973 to 1988, he was employed by the University of Rennes, as an Assistant and then Assistant Professor. He worked for CELAR Ministry of Defense (1985–1987) on radar signal processing. Now he is a Professor with the Ecole polytechnique de l'université de Nantes, Nantes France and in charge of the Radar Research Team in the Institut

de Recherche en Electrotechnique et Electronique de Nantes Atlantique (IREENA) Laboratory. His fields of interest are the radar polarimetry, adaptive antennas, electronics systems. These activities are done in close collaboration with other public research organizations and industry.

Dr. Saillard is member of the Electromagnetic Academy. He is the organizer of JIPR'90, '92, '95 and '98.